
Doctoral Dissertations

Student Theses and Dissertations

1971

An age hardening study of magnesium-thorium-manganese alloys

Kuldip Singh Chopra

Follow this and additional works at: https://scholarsmine.mst.edu/doctoral_dissertations

 Part of the [Metallurgy Commons](#)

Department: Materials Science and Engineering

Recommended Citation

Chopra, Kuldip Singh, "An age hardening study of magnesium-thorium-manganese alloys" (1971). *Doctoral Dissertations*. 1838.

https://scholarsmine.mst.edu/doctoral_dissertations/1838

This thesis is brought to you by Scholars' Mine, a service of the Missouri S&T Library and Learning Resources. This work is protected by U. S. Copyright Law. Unauthorized use including reproduction for redistribution requires the permission of the copyright holder. For more information, please contact scholarsmine@mst.edu.

AN AGE HARDENING STUDY OF MAGNESIUM -
THORIUM - MANGANESE ALLOYS

By

KULDIP SINGH CHOPRA, 1934-

A DISSERTATION

Presented to the Faculty of the Graduate School of the

UNIVERSITY OF MISSOURI-ROLLA

In Partial Fulfillment of the Requirements for the Degree

DOCTOR OF PHILOSOPHY

in

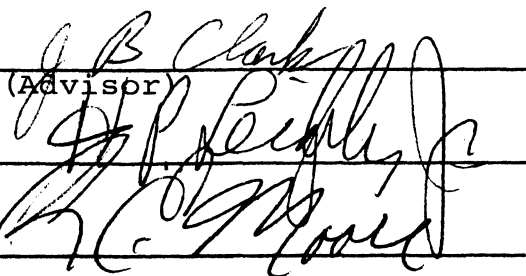
METALLURGICAL ENGINEERING

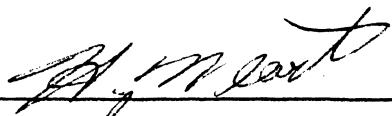

1971

T2612

29 pages

c.1


(Advisor)

202892

PUBLICATION DISSERTATION OPTION

This dissertation has been prepared in the style utilized by the Acta Metallurgica. Pages iii and 1 - 27 will be submitted for publication in that journal.

ABSTRACT

The age hardening processes in Mg-3.5 wt.% Th-1.0 wt.% Mn and Mg-1.0 wt.% Th-1.0 wt.% Mn alloys have been studied by light and electron microscopy, and by electron and X-ray diffraction. At aging temperatures of 300°C and below, G.P. zone formation rapidly hardens these alloys followed by the precipitation of disc shaped plates during overaging. During aging above 300°C, no G.P. zones form and the disc shaped precipitate grows to very large sizes. The combined results of X-ray and electron diffraction indicate that the disc shaped precipitate has a Mg_3Cd (DO_{19}) type structure. The basal plane of the Mg_3Th discs lie parallel to the matrix basal plane which is also the habit plane of this precipitate. Basal slip and $\{10\bar{1}2\}$ twinning, the principal deformation modes, shear the G.P. zones but not the Mg_3Th discs.

PREFACE

The author wishes to acknowledge his sincere appreciation for the guidance and patience of his advisor Professor J. B. Clark.

TABLE OF CONTENTS

	Page
PUBLICATION DISSERTATION OPTION.....	ii
ABSTRACT.....	iii
PREFACE.....	iv
LIST OF ILLUSTRATIONS.....	vi
LIST OF TABLES.....	viii
I. INTRODUCTION.....	1
II. EXPERIMENTAL PROCEDURE.....	3
III. RESULTS.....	6
A. AGE HARDENING AND PRECIPITATE STRUCTURES.....	6
B. THE STRUCTURE OF INTERMETALLIC PRECIPITATE.....	7
C. ORIENTATION RELATIONSHIP AND HABIT OF THE DISC SHAPED Mg ₃ Th PRECIPITATE.....	10
D. EFFECT OF DEFORMATION.....	11
IV. DISCUSSION.....	13
REFERENCES.....	17
VITA.....	27
APPENDIX I - TABLE SHOWING CORRELATION BETWEEN AGING TIME AND HARDNESS AT VARIOUS TEMPERATURES FOR HM31 (Mg-3.5 wt.% Th-1.0 wt.% Mn) ALLOY.....	28
APPENDIX II - TABLE SHOWING CORRELATION BETWEEN AGING TIME AND HARDNESS AT VARIOUS TEMPERATURES FOR HM11 (Mg-1.0wt.% Th-1.0 wt.% Mn) ALLOY.....	29

LIST OF ILLUSTRATIONS

Figures	Page
1. Age hardening of HM31 alloy as a function of aging temperature.....	18
2. Age hardening of HM11 alloy as a function of aging temperature.....	19
3. Fine G.P. zone dispersion in HM31 alloys. S.T. + 1 hour at 260°C. X117,000.....	20
4. Structure of HM31 alloy at maximum hardness for aging at 260°C. A mixture of fine Mg ₃ Th discs is surrounded by fine G.P. zones. S.T. + 19 hours at 260°C. X51,000.....	20
5. Structure of overaged HM31 alloy consisting of Mg ₃ Th discs in G.P. zone free matrix. S.T. + 12 days at 260°C. X59,000.....	21
6. Structure of overaged HM31 alloy consisting of Mg ₃ Th discs in G.P. zone free matrix. S.T. + 11 days at 300°C. X45,000.....	21
7. Electron diffraction pattern along [0001] of matrix of HM31 alloy with well developed disc shaped plates. Note the hexagonal array of matrix spots surrounding a similar array of precipitate spots.....	22
8. Very large discs of Mg ₃ Th precipitate lying in the basal plane of the matrix of HM31 alloy. Plane of foil is (0001). S.T. + 9 hours at 400°C. X33,000.....	22
9. Cross section of large Mg ₃ Th discs lying in basal plane of the matrix of HM31 alloy as seen from the foil in prism orientation. S.T. + 9 hours at 400°C. X20,000.....	23
10. Mg ₃ Th precipitate in HM11 alloy. Note the disc nature of the precipitate. S.T. + 31 days at 260°C. X20,000.....	24
11. Mg ₃ Th precipitate in HM11 alloy. S.T. + 10 hours at 400°C. X20,000.....	24
12. Large aligned discs of Mg ₃ Th precipitate in HM31 alloy. S.T. + deformation + 9 hours at 400°C. X42,000.....	25

LIST OF ILLUSTRATIONS (CONTINUED)

Figures	Page
13. Mg_3Th precipitate in HM31 alloy retarding growth of $\{10\bar{1}2\}$ type twin. Dark field image. S.T. + 28 days at 300°C + deformation. X30,000.....	25

LIST OF TABLES

Table	Page
I. Table showing the calculated d spacings of proposed hexagonal _o (DO ₁₉) type cell of Mg ₃ Th with a = 5.56 Å, c = 31.2 Å. X-ray and electron diffraction d values and Rostoker's reported values of Mg ₄ Th phase.....	26
A. APPENDIX I - Table showing correlation between aging time and hardness at various temperatures for HM31 (Mg-3.5 wt.% Th-1.0 wt.% Mn) alloy.....	28
A. APPENDIX II - Table showing correlation between aging time and hardness at various temperatures for HM11 (Mg-1.0 wt.% Th-1.0 wt.% Mn) alloy.....	29

I. INTRODUCTION

The magnesium-thorium system forms the basis of a series of alloys which maintain high strength at temperatures up to 350°C. In commercial alloys, magnesium-thorium alloys are modified by ternary additions of either zirconium (HK alloys)/or manganese (HM alloys). The Zr addition was made for the purpose of grain size control. However, this study and recent work shows the zirconium and manganese have direct influence on the strengthening processes in these alloys.

At the beginning of the present study, several investigations (1,2,3) had been undertaken on the Mg-Th-Zr (HK) alloys; however, no work had been reported on the Mg-Th-Mn (HM) alloys. Accordingly, the present study was undertaken on two alloys, Mg-3.5 wt.% Th-1 wt.% Mn alloy and Mg-1.0 wt.% Th-1.0 wt.% Mn. In this paper the first alloy above will be referred to as HM31 alloy and the second as HM11 alloy. It was thought that the different ratios of thorium to manganese would result in different precipitation processes, however, the precipitation sequence of both alloys was found to be identical. The details of the precipitation reactions and hardening mechanisms in these alloys were to be determined principally by light and transmission electron microscopy, and x-ray and electron diffraction.

In the most recent investigation of the Mg-Th phase diagram, Yamamoto and Rostoker⁽⁴⁾ designate the phase in

equilibrium with magnesium solid solution as $\text{Mg}_{23}\text{Th}_6$ (Mg_4Th) to which those investigators ascribed an f.c.c. structure with a lattice parameter of 14.37\AA . As shown below, this phase precipitates during the overaging of both Mg-Th-Mn alloys selected for study. Since there is no evidence of any third precipitate phase in the aged alloys, at age hardening temperatures, the above alloys lie in the (magnesium solid solution + Mg_4Th) phase field of the Mg-Th-Mn phase diagram.

In an early investigation of binary Mg-Th and Mg-Th-Zr alloys Murakami, Kawano and Tamura⁽²⁾ report the formation of G.P. zones and the precipitation of a transition lattice " Mg_2Th " reported by Sturkey⁽¹⁾. The Mg_2Th transition lattice was not seen in the present study. In a more recent investigation of precipitation in a binary Mg-Th alloy, Noble and Crook⁽⁵⁾ report the precipitation of another transition lattice with the Mg_3Cd (DO_{19}) type superstructure ($a = 6.4\text{\AA}$, $c = 5.2\text{\AA}$) in the form of plates on the prism plane of the matrix. With overaging, plates of f.c.c. Mg_4Th are reported to form on the basal plane of the matrix. The two precipitates appear to nucleate and grow independently.

It is shown below that precipitation in both the HM31 and HM11 alloys selected for study differs from that reported for the binary alloys^(2,5) and also that of Mg-Th-Zr alloys^(1,3). Evidently, the addition of manganese greatly modifies the precipitation processes.

II. EXPERIMENTAL PROCEDURE

The two alloys studied in the investigation contained 3.5 wt.% Th and 1 wt.% Mn, similar to the commercial magnesium alloy HM31A and 1.0 wt.% Th and 1 wt.% Mn. Foil stock (1-3/4" wide and 0.010" thick) and sheet stock (1-3/4" wide by 1/8" thick) of both alloys were supplied by the Dow Metal Products Company through the courtesy of S. L. Couling.

Prior to heat treatment, each sheet of the alloy stock was examined in the electron microscope for the presence of thorium hydride. Thorium in magnesium alloys can readily combine with hydrogen to form stable hydrides (ThH_2 and Th_4H_{15}) to such an extent that without special protection during heat treatments all the thorium in the alloy can be converted to hydride leaving none for precipitation hardening. To prevent loss of thorium by hydride formation during solution treatment, alloy specimens were first sandwiched between sheets of magnesium foil and then wrapped in molybdenum foil. This composite along with a small quantity of Ti-Zr getter was sealed in pyrex vials under high purity dry argon. The foil composite and the getter material were separated to opposite ends of the pyrex vial. The end of the vial containing the getter was then placed in a furnace at 700°C for 12 hours. This treatment purged the argon of remaining traces of hydrogen. Foil wrapping of the composite prevents attack of the pyrex container by the magnesium during solution heat treatment.

The solution treatment consisted of an eight hour anneal at 590°C, followed by a water quench. Aging treatments were carried out in pyrex vials under high purity dry argon at 260, 280, 300, 350 and 400°C and were terminated by a water quench.

Hardness tests were made at room temperature immediately after quenching from aging temperatures, using the E scale of Rockwell hardness testing machine. Each reported value is the average of at least 4 measurements having a maximum spread of ± 2 points.

Transmission electron microscopy and diffraction on a Hitachi HU-11A electron microscope was used to determine the precipitation process. Both electrolytic and chemical thinning procedures were developed. In order to shorten the thinning time, sheet and foil specimens were thinned chemically down to a 0.001" first in a solution of concentrated nitric acid (30% by volume) plus absolute ethyl alcohol. The final thinning was done by the window method in 85% orthophosphoric acid at room temperature and applied voltage of 15 to 20 volts. At the completion of thinning, the specimen was rinsed in a stream of methyl alcohol and dried. Before examination, it was found necessary to clean the thinned specimen in a solution of equal parts of 85% orthophosphoric acid and absolute ethyl alcohol maintained at -10 to -15°C. The specimen was agitated in this solution for 2 to 5 minutes then rinsed in methyl alcohol and air dried.

X-ray diffraction was done with a 114 mm diameter Debye-Scherrer camera using Cu radiation with either a nickel filter or a quartz crystal monochromator. Filing could not be used for preparation of the X-ray powder sample because the filing appeared to induce precipitation in solution treated specimens. Therefore, the powder samples were prepared by the "sliver" technique reported by Shapiro⁽⁶⁾ in which the Debye-Scherrer specimen consists of a series of fine slivers cut with a sharp scalpel from the thin edge of a transmission specimen window. With this technique, solution treated specimens showed no evidence of strain induced precipitation and the matrix lattice showed suitable distortion due to solute.

III. RESULTS

A. AGE HARDENING AND PRECIPITATE STRUCTURES

The age hardening response of the two Mg-Th-Mn alloys is given in figures 1 and 2. In general, the hardening curves are characterized by a very rapid rise in hardness at low aging times, followed by an extended plateau and a slow decay in hardness. Note also that the hardening curves do not follow the classical pattern for a one precipitate hardening system. For example, in figure 2, the peak hardness for aging at 300°, 280° and 260°C should classically be at successively longer times, rather than the inverse relationship shown. In both alloys, the hardening curves for aging at 300°C, and below, suggest a two stage precipitation process. The very rapid rise is characteristic of G.P. zone formation and the long plateau and slow decay in hardness suggest precipitation of a second phase and its growth during overaging.

Transmission electron microscopy confirmed the two stage precipitation in these alloys. G.P. zones formed rapidly during aging below 300°C. The G.P. zone dispersion in the higher thorium alloy after 1 hour at 260°C is shown in figure 3. Electron diffraction detected no other precipitate but did indicate that the matrix lattice was strained. In all cases, the presence of G.P. zones correlated with a strained matrix.

After about 8 hours of aging at 260°C, in the HM31

alloy, a second precipitate designated Mg_3Th , formed as discs on the basal plane of the matrix. The structure at maximum hardness for aging at $260^{\circ}C$ shown in figure 4, consisted of a matrix of very fine intermetallic discs and G.P. zones. With further aging the intermetallic discs grow with concomitant dissolution of G.P. zones and decay in hardness as shown in figure 5. With the same aging time at $300^{\circ}C$, as shown in figure 6, the disc size increases. The precipitate sequence (G.P. zones followed by intermetallic discs) was identical during aging at 280° and $300^{\circ}C$ except precipitation was more rapid and the disc shaped precipitates attained a little larger size with prolonged aging. Except for smaller amounts of precipitates, the same precipitation sequence was seen in the HM11 alloy.

No G.P. zones were observed in specimens of either alloy aged at 350° and $400^{\circ}C$. Therefore, for these alloys, the G.P. zones solvus must be between 300° and $350^{\circ}C$. As shown in figure 3, aging at 350° and $400^{\circ}C$ produces only moderate hardening which quickly decays with time. At these temperatures disc shaped precipitates form rapidly and may grow to very large sizes, resulting in rapid loss of hardness. (See figures 8 and 9).

B. THE STRUCTURE OF THE INTERMETALLIC PRECIPITATE

Yamamoto and Rostoker⁽⁴⁾ from Debye-Scherrer work

reported that the phase in equilibrium with the magnesium solid solution could be indexed as a f.c.c. structure with a lattice parameter equal to 14.37 \AA . From quantitative metallography and density determinations, these workers assigned the composition Mg_5Th ; later Sturkey⁽¹⁾ assigned the composition Mg_4Th to the phase. In the present work, thin sliver, Debye-Scherrer X-ray diffraction of both Mg-Th-Mn alloys aged to precipitate large disc precipitates yields x-ray patterns identical to these reported by Yamamoto and Rostoker⁽⁴⁾. Thus, the disc shaped precipitates are the Mg_5Th phase reported to be the intermetallic phase in equilibrium with the magnesium solid solution. However, in the course of the present investigation, many single crystal patterns for this precipitate were taken by selected area electron diffraction along different crystal axes. In all cases, the zero order of the Laue pattern could not be accounted for by the above f.c.c. structure. Such a case is shown in figure 7. The foil normal is parallel to the $[0001]$ direction of the matrix and the hexagonal array of $(10\bar{1}0)$ spots characteristic of the basal plane is seen. Within this array of matrix spots, a hexagonal array of spots, confirmed as coming from the disc shaped precipitate by dark field imaging is seen. The hexagonal array and the f.c.c. structure assigned by Yamamoto and Rostoker suggests that these are (220) spots of the (111) plane of the f.c.c. disc precipitate. Thus it could be concluded

that the (111) plane of the f.c.c. precipitate is parallel to the basal plane of the matrix. However, such is not the case, because these spots do not have the correct spacings (5.09Å) to be the (220) spots of a f.c.c. lattice with a parameter of 14.37Å. These spots have a spacing of 4.82Å. It appears that the precipitate is not f.c.c. Single crystal patterns of disc shaped precipitate from other matrix planes, $(10\bar{1}0)$, $(\bar{1}2\bar{1}3)$, $(\bar{1}2\bar{1}2)$ also could not be analyzed on the basis of the f.c.c. lattice above. Also, additional interplanar spacings which could not be detected by X-ray diffraction were obtained from the selected area diffraction patterns. Table I lists the d values for the precipitate obtained from both X-ray and electron diffraction. Comparison of the X-ray spacings with these reported by Yamamoto and Rostoker for Mg_5Th shows complete agreement. However, the extra spacings derived from electron diffraction precluded analysis as a simple f.c.c. structure for the phase. As shown in Table I, all the d values can be indexed by ascribing a Mg_3Cd type (DO_{19}) structure with $a = 5.56\text{Å}$, $c = 31.2\text{Å}$ to this precipitate. Single crystal patterns of the precipitate obtained from foil with the following matrix planes (0001) , $(10\bar{1}0)$, $(\bar{1}2\bar{1}3)$ and $(\bar{1}2\bar{1}2)$ were analyzed using the above structure. The calculated angles and spacings of the patterns for this cell agreed with these obtained experimentally. Thus, the intermetallic disc shaped precipitates have a hexagonal structure of the Mg_3Cd type (DO_{19}) and a composition close

to Mg_3Th . Noble and Crook⁽⁵⁾, and Mushovic and Stoloff⁽³⁾ have proposed this structure for precipitate in binary Mg-Th and Mg-Th-Zr alloys respectively.

C. ORIENTATION RELATIONSHIP AND HABIT OF THE DISC SHAPED Mg_3Th PRECIPITATE

The orientation relationship between the Mg_3Th precipitate and the matrix is readily apparent in figure 7, in which the diffraction pattern of the basal plane of the matrix is adjacent to that of the Mg_3Th precipitate with a 30° relation of the latter above the c axis. The orientation relationship is:

$$\begin{aligned} (0001)_{\text{Mg}} // (0001)_{\text{Mg}_3\text{Th}} \\ [10\bar{1}0]_{\text{Mg}} // [11\bar{2}0]_{\text{Mg}_3\text{Th}} \end{aligned}$$

This relationship was confirmed also with the following matrix planes $(10\bar{1}0)$, $(\bar{1}2\bar{1}3)$ and $(\bar{1}2\bar{1}2)$.

The habit plane of the Mg_3Th discs in the HM31 alloy is shown in figure 8, which shows the very large discs that may be grown upon aging at 400°C lying on the basal plane of the matrix. Confirmation of the basal plane habit is given in figure 9, which shows the cross section of the discs when viewed from a prism orientation. In the HM11 alloy the Mg_3Th precipitate forms in very fine discs at aging temperatures below 300°C . But at higher aging temperatures, this precipitate tends to have a more irregular shape.

Two dispersions of this phase are shown in figures 10 and 11. The irregular form of the Mg_3Th phase is especially marked with aging at 400°C . The structure and orientation of the phase is identical to that of Mg_3Th in the HM31 alloy.

D. EFFECT OF DEFORMATION

Deformation of these alloys after solution treatment and prior to aging does not markedly increase the amount of the Mg_3Th precipitate for a given aging time. Thus, the Mg_3Th precipitate in these HM alloys does not nucleate on dislocations as reported for the binary Mg-3.0 wt.% Th alloy⁽⁵⁾. However, as in Mg-Zn alloys⁽⁷⁾ precipitation of the intermetallic phase seems to occur more rapidly within the $\{10\bar{1}2\}$ twins. Also, as shown in figure 12, there is some tendency to be aligned in $[\bar{1}\bar{1}23]$ directions. Here also, the very large size of the Mg_3Th discs indicated that nucleation is low and not enhanced by deformation.

The principal deformation modes operating in these alloys were determined by trace analysis of the deformation markings on pre-polished sheet specimens. The specimens were solution treated, aged under inert atmosphere to protect the polish, then given a 4% compression strain parallel to the rolling direction. Light microscopy of both alloys revealed only two major deformation mechanisms—basal slip, and $\{10\bar{1}2\}$ twinning regardless of heat treatment. No cross slip was observed. Also the twin bands reported

by Paskak and Couling⁽⁸⁾ for rolled HK31 alloy were not seen. However, in the present study, the HM alloys were not deformed by rolling and twin bands might form with rolling.

Transmission electron microscopy was used to determine the interaction of slip dislocations and $\{10\bar{1}2\}$ twinings with precipitate structures. Slip dislocation appears to cut the G.P. zones although interaction is difficult to determine because of the small size of the zones. The Mg_3Th precipitate is not cut by slip dislocations. Although not oriented for efficient blocking of basal slip, the Mg_3Th precipitate does appear to induce the formation of dislocations tangles which would raise the flow stress.

Twins of the $\{10\bar{1}2\}$ type did not shear the Mg_3Th precipitates which tended to retard growth of the twins. In figure 13, the twin-matrix interface is ragged due to circumvention of the precipitate by the twin. However, suppression of $\{10\bar{1}2\}$ twins by precipitation was not as marked as in Mg-Al alloys⁽⁹⁾.

IV. DISCUSSION

At age hardening temperatures, both ternary alloys lie in the (magnesium solid solution + Mg_3Th) phase field that adjoins the Mg-Th side of the Mg-Th-Mn phase diagram. In this study neither α Mn, nor any intermetallic compound other than Mg_3Th were seen regardless of age hardening heat treatment. However, manganese in solution must have an influence on the precipitation processes because the precipitation in these Mg-Th-Mn alloys differs considerably from those reported for either the binary Mg-Th alloys or Mg-Th-Zr alloys.

The formation of G.P. zones in these Mg-Th-Mn alloys during aging at 300°C and below is the main strengthening reaction of these Mg-Th-Mn alloys. The G.P. zones are very stable and strength is maintained for long periods even after the formation of some Mg_3Th precipitate. However, the structure and composition of the G.P. zones remains unknown. Sturkey⁽¹⁾ points out that high chemical affinity of thorium for hydrogen and the relatively high solubility of hydrogen in magnesium provides a basis for an explanation of the low mobility of thorium and the stability of Mg-Th alloys. The stability of the G.P. zones in these HM alloys may be explained on similar grounds. The high Mn-H affinity may also influence the diffusion of thorium and the stability of the zones by the formation of Th-Mn complexes held together by manganese. However, other tools, such as

careful internal friction studies are needed to determine the structure and composition of these G.P. zones.

The nucleation site for the Mg_3Th precipitates is not known. But, the small size of the Mg_3Th precipitates at aging temperatures below the G.P. zone solvus, which lies between 300 and 350°C, compared to the very large discs above the solvus, suggest that the G.P. zones act as nucleating sites for the intermetallic precipitate as in Al-Mg-Zn alloys.⁽¹⁰⁾

In the HM31 the Mg_3Th discs appear to remain coherent at all temperatures studied and for aging times up to 30 days. In no case did these discs coarsen and agglomerate. The formation and stability of the Mg_3Th discs can be explained on the basis of lattice matching. The hexagonal lattices of matrix and precipitate match best when planes are parallel. With this orientation two cells of the matrix match well with one cell of the Mg_3Th precipitate. In contrast along the c axis, the disregistry is very large. The reason for the irregular shape and smaller size of the Mg_3Th in the HM11 alloy at higher aging temperatures is not known.

As noted above, the structure of the intermetallic precipitate in these alloys is the Mg_3Cd type (DO_{19}) with $a_0 = 5.56\text{\AA}$ and $c = 31.20\text{\AA}$. Simultaneously with the present study, Stratford⁽¹¹⁾ independently undertook a study of precipitation in HM21 alloy. He also could not analyze the electron diffraction pattern of the intermetallic precipitate

on the basis of the f.c.c. Mg_4Th structure proposed by Yamamoto and Rostoker or the $\text{Mg}_2\text{Th}^{(4)}$ structure proposed by Sturkey⁽¹⁾. Independently Stratford⁽¹¹⁾ derived the Mg_3Cd (DO_{19}) type structure noted above, for the inter-metallic precipitate.

During the course of this investigation, Noble and Crook⁽⁵⁾ published their study of precipitation in a binary Mg-3.0 wt.% Th alloy. They report precipitation in this alloy to be a two stage process. First, platelets of a transition structure (with Mg_3Cd type structure), designated β'' , formed on the prism planes of the matrix followed by independent precipitation of the equilibrium phase designated Mg_4Th (with a f.c.c. structure) on the basal plane of the matrix. The equilibrium precipitate formed as large black agglomerates. Note that in the binary alloy, the structure of the transition lattice has the Mg_3Cd (DO_{19}) type structure for the disc shaped precipitate of the HM31 and HM11 alloys. These precipitates are undoubtedly the same Mg_3Th phase. But the habit plane of this precipitate differs in the binary alloys, the Mg_3Th forms on the prism planes of the matrix; in the HM alloys on the basal plane. It is difficult to visualize the effect of the manganese addition on this change in habit. Addition of manganese to magnesium does decrease slightly the a as well as the c parameter⁽¹²⁾ but not enough to affect the disregistry sufficiently to change the habit plane of the Mg_3Th precipitate.

The large dark precipitate seen in the binary alloy after prolonged aging and designated as β , the equilibrium precipitate Mg_4Th by Noble and Crook⁽⁵⁾ is not seen in the Mg-Th-Mn alloys. Noble and Crook⁽⁵⁾ propose that the Mg_3Th precipitate is a transition precipitate whereas the present investigation shows that Mg_3Th plates are equilibrium. In the Mg-Th-Mn there is no evidence that, Mg_3Th is a transition lattice but rather that the Mg_3Th discs are an equilibrium precipitate.

REFERENCES

1. L. Sturkey, T. AIME 218, (1960), p. 466.
2. Y. Murakami, O. Kawano and H. Tamura, Mem. Fac. Eng. Kyoto University, 24 (1962), p. 411.
3. J. N. Mushovic and N. Stolloff, T. Japan Inst. Metals, 9 (Suppl.), 1968, 360.
4. A. S. Yamamoto and W. Rostoker, T. ASM, 50 (1958), p. 1090.
5. B. Noble and A. Crook, J. Inst. of Metals, 98, (1970), p. 375.
6. J. M. Shapiro, "Kinetics of Discontinuous Precipitation in Copper-Indium Alloys", Ph.D. Thesis, McMaster University, 1966.
7. J. B. Clark, Acta Met. 13, 1281 (1965).
8. J. F. Pashak, S. L. Couling and L. Sturkey, T. ASM, 51 (1959), p. 94.
9. J. B. Clark, Acta Met. 16, 141 (1968).
10. G. W. Lormier and R. B. Nicholson, Acta Met., vol. 14, 1966, p. 1009.
11. D. J. Stratford, Private communication.
12. R. S. Bush, T. AIME 188, (1956), p. 1460.

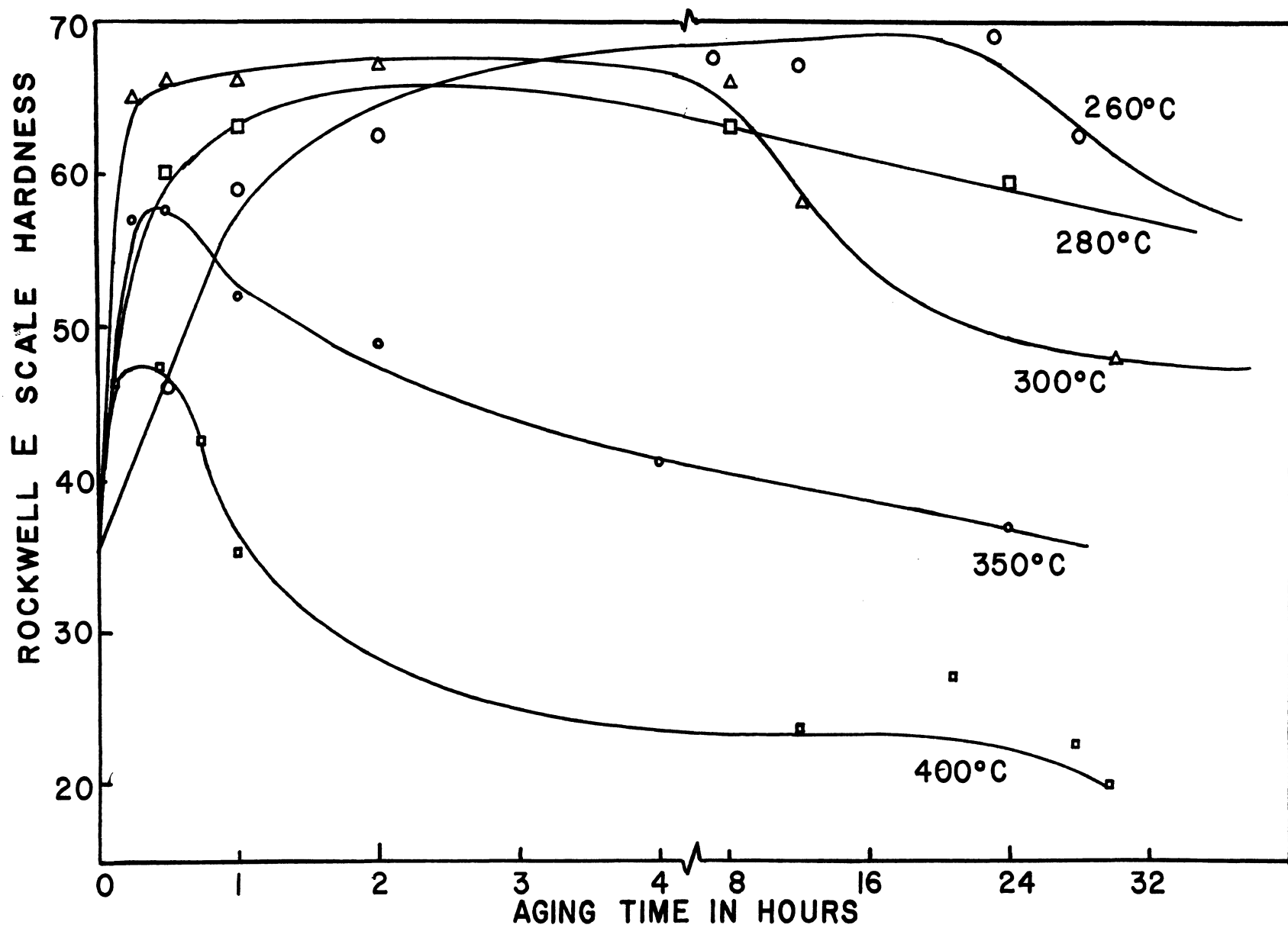


Figure 1: Age Hardening of HM31 Alloy as a Function of Aging Temperature

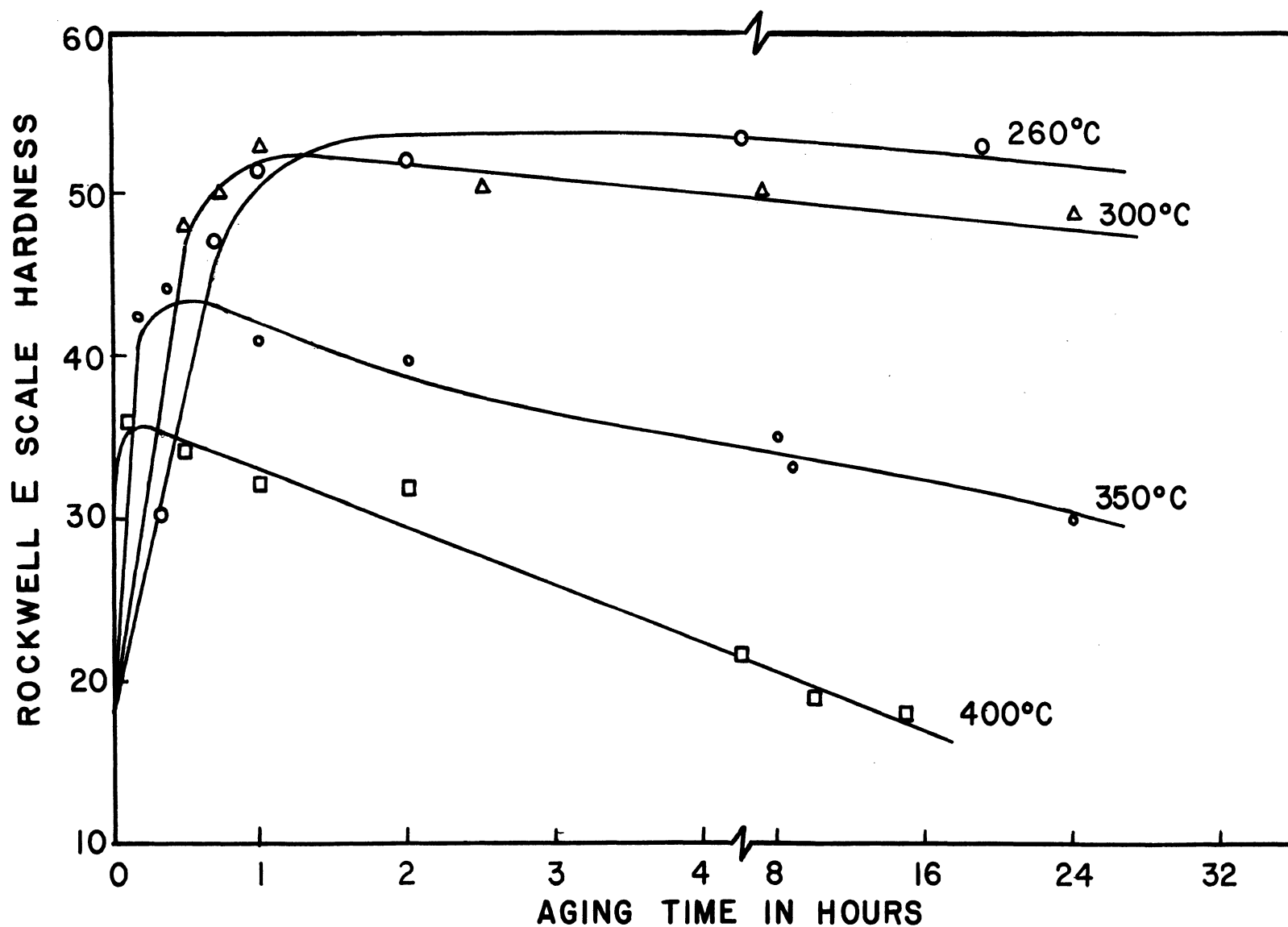


Figure 2: Age Hardening of HM11 Alloy as a Function of Aging Temperatures

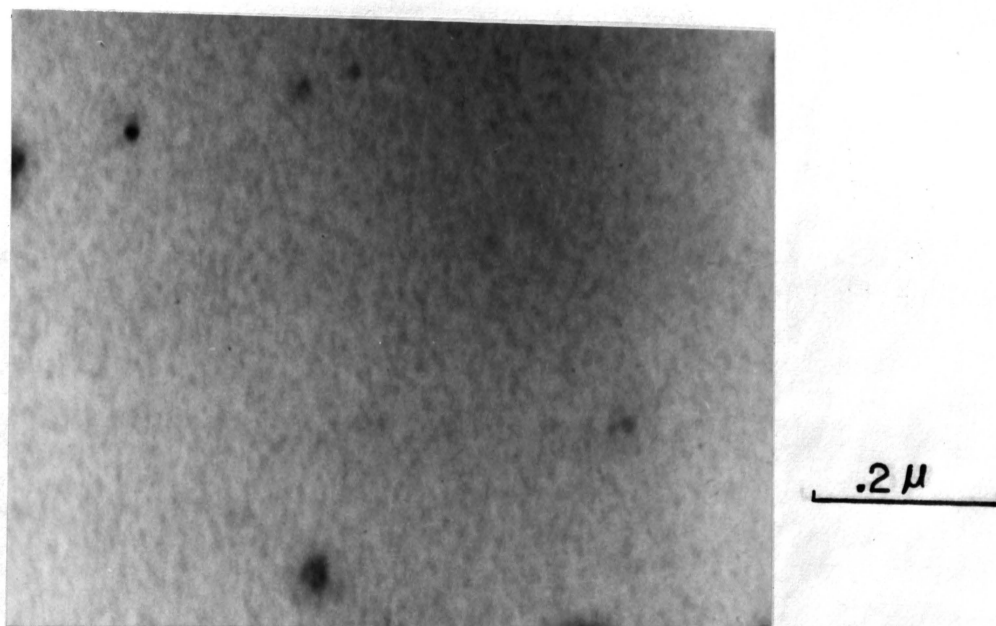


Figure 3. Fine G.P. zone dispersion in HM31 alloys. S.T. + 1 hour at 260°C. X117,000.

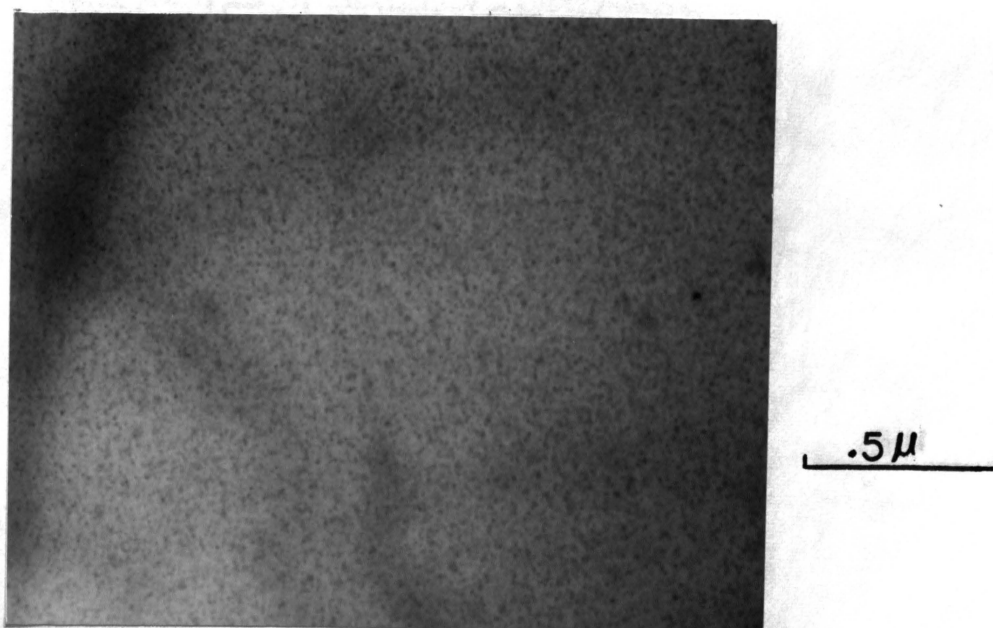


Figure 4. Structure of HM31 alloy at maximum hardness for aging at 260°C. A mixture of fine Mg_3Th discs is surrounded by a fine dispersion of G.P. zones. S.T. + 19 hours at 260°C. X51,000.

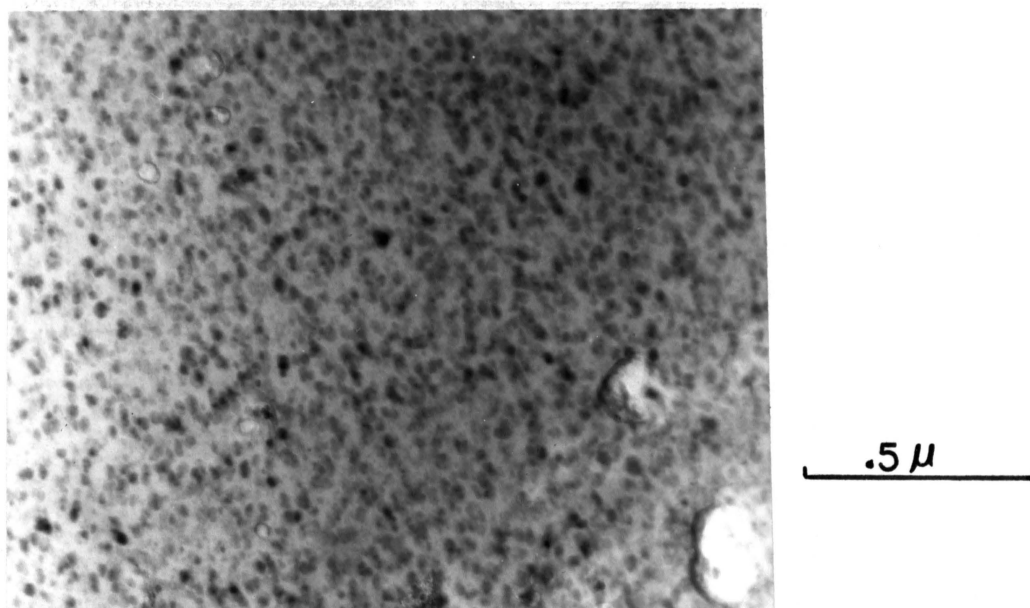


Figure 5. Structure of overaged HM31 alloy consisting of Mg_3Th discs in G.P. zone free matrix. S.T. + 12 days at $260^\circ C$. X59,000.

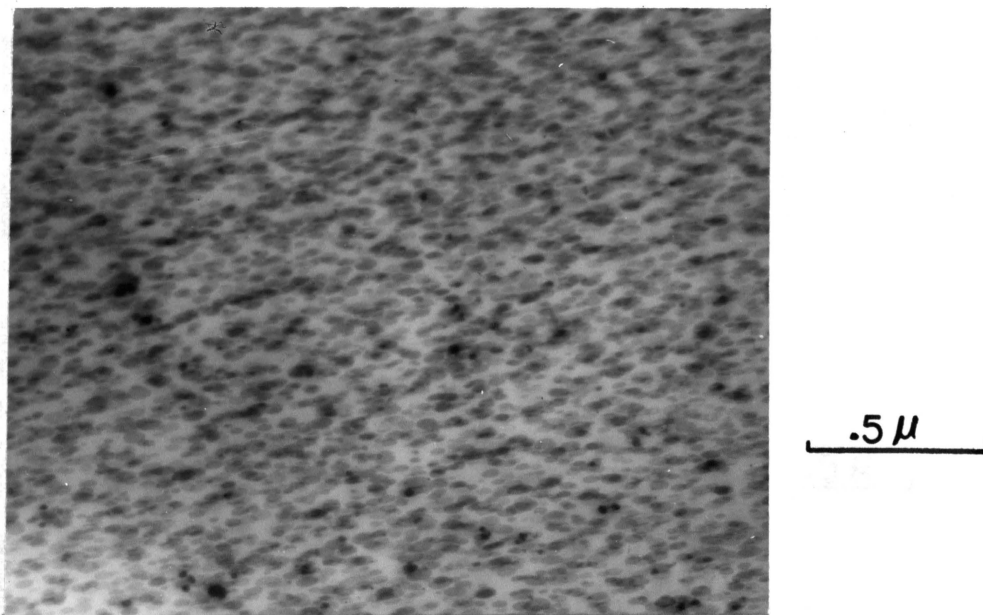


Figure 6. Structure of overaged alloy consisting of Mg_3Th discs in G.P. zone free matrix. S.T. + 11 days at $300^\circ C$. X45,000.

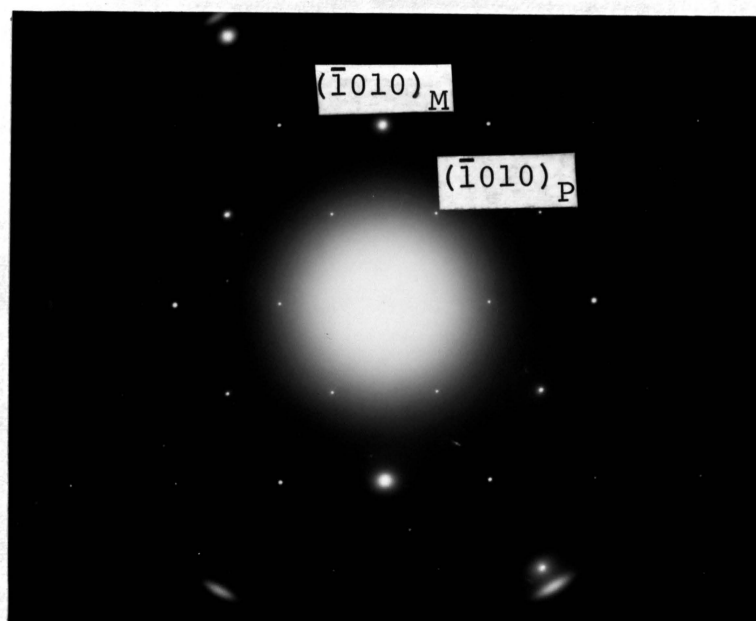


Figure 7. Electron diffraction pattern along $[0001]$ of matrix of HM31 alloy with well developed disc shaped plates. Note the hexagonal array of matrix spots surrounding a similar array of precipitate spots.

Figure 8.

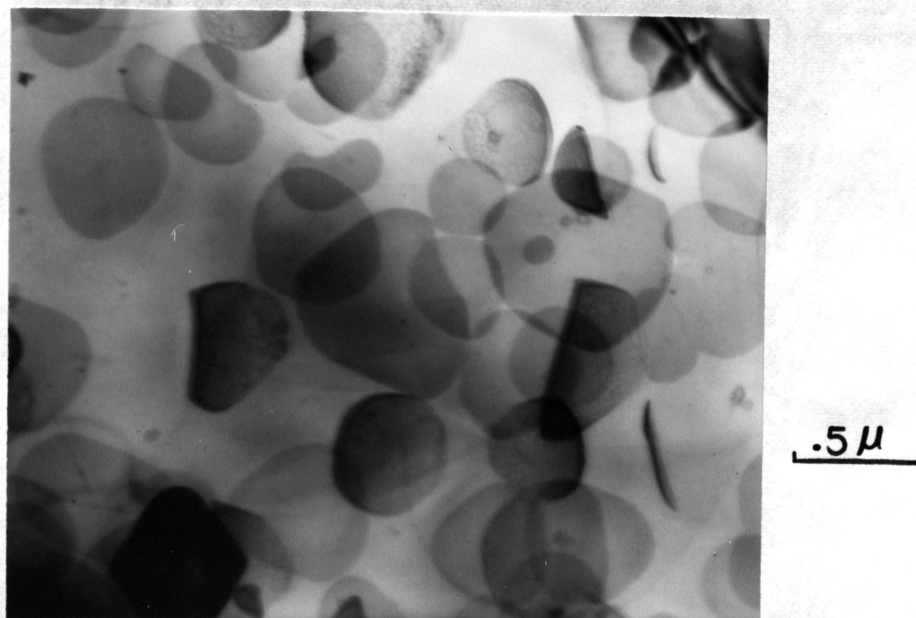


Figure 8. Very large discs of Mg_3Th precipitate lying in the basal plane of the matrix of HM31 alloy. Plane of foil is (0001) . S.T. + 9 hours at $400^\circ C$. X33,000.



Figure 9. Cross section of large Mg_3Th discs lying in basal plane of the matrix of HM31 alloy as seen from foil in prism orientation. S.T. + 9 hours at $400^\circ C$. X20,000.

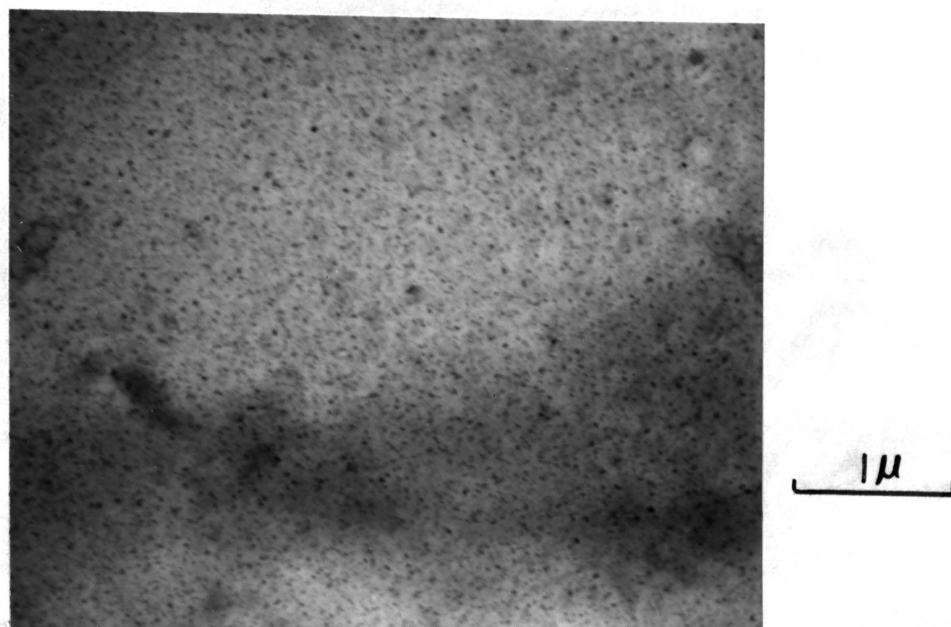


Figure 10. Mg_3Th precipitate in HM11 alloy. Note the disc nature of the precipitate. S.T. + 31 days at 260°C. X20,000.

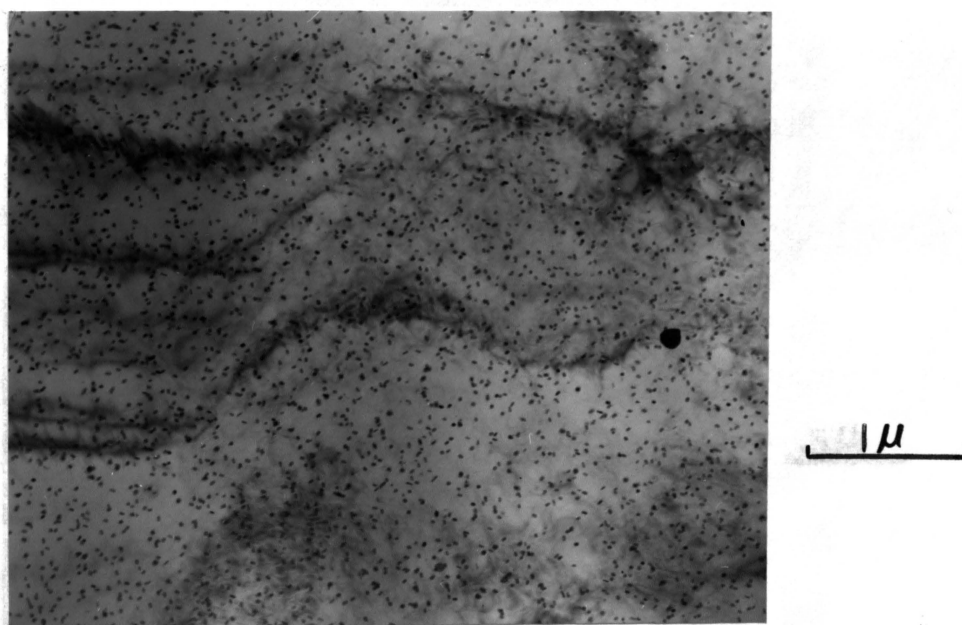


Figure 11. Mg_3Th precipitate in HM11 alloy. S.T. + 10 hours at 400°C. X20,000.

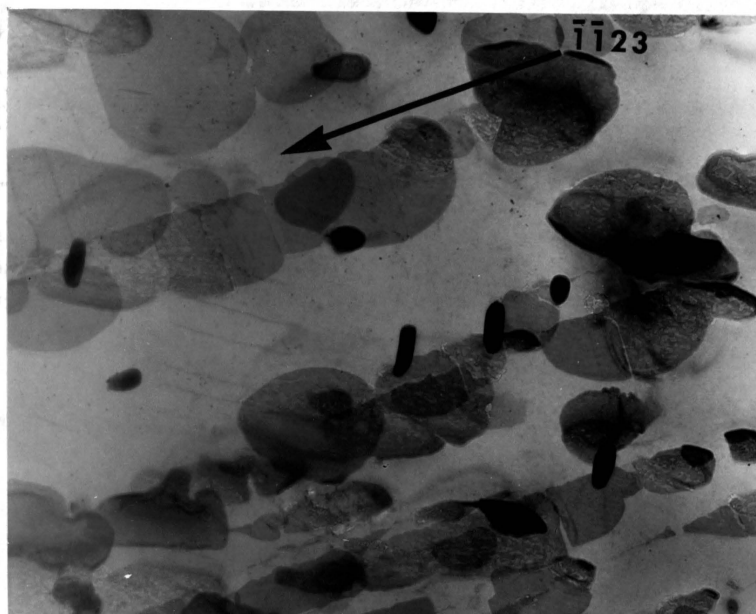


Figure 12. Large aligned discs of Mg₃Th precipitate in HM31 alloy. S.T. + deformation + 9 hours in 400°C. X42,000.

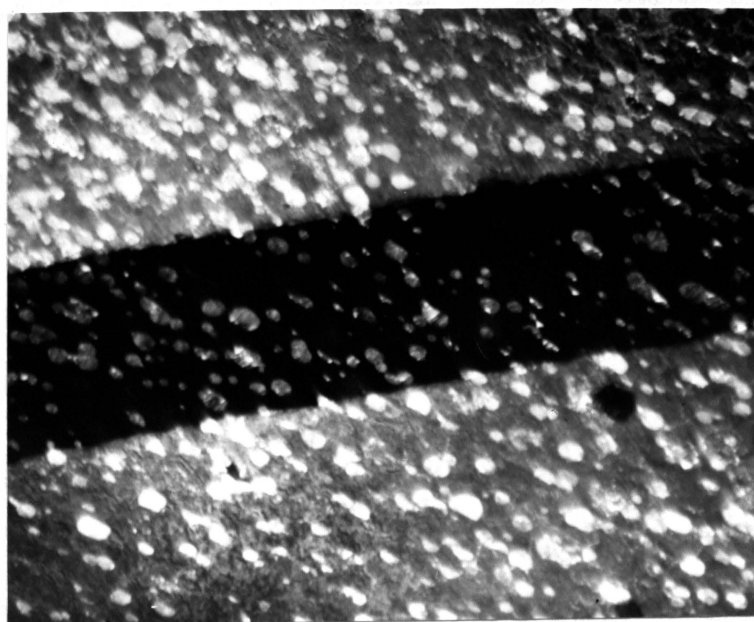


Figure 13. Mg₃Th precipitate in HM31 alloy retarding growth of {1012} type twin. Dark field image. S.T. + 28 days at 300°C + deformation. X30,000.

TABLE I

Table showing the calculated d spacings of proposed hexagonal (DO_{19}) type cell of Mg_3Th with $a = 5.56 \text{ \AA}$, $c = 31.2 \text{ \AA}$. X-ray and electron diffraction d values and Rostoker's reported values of Mg_4Th phase.

hkl	Calculated 'd' spacing of cell $a=5.56 \text{ \AA}$ $c=31.2 \text{ \AA}$	'd' spacing from electron and X-ray diffraction pattern	'd' spacing Rostoker f.c.c. (Mg_4Th) $a=14.37 \text{ \AA}$
002	15.600	8.34*S.L. of (104)	8.34
004	7.800	7.22*S.L. of (106)	7.20
		5.09*S.L. of (114)	5.08
100	4.815	4.82 [†]	
101	4.750	4.75 [†]	
102	4.600	4.60 [†]	
103	4.369	4.34 [†]	4.33
104	4.120	4.12* [†]	4.15
105	3.812	3.80 [†]	
106	3.533	3.54 [†]	3.60
107	3.270	3.30*	3.30
108	3.030	2.94*	2.94
110	2.780	2.77* [†]	2.77
114	2.618	2.54* [†]	2.54
201	2.400	2.42* [†]	2.40

*X-ray Diffraction

†Electron Diffraction

VITA

The author was born on November 5, 1934, in Karachi, Pakistan. He got his Bachelor of Science Degree from India in 1957. He came to United States in 1959. He received his B.S. and M.S. in Metallurgical Engineering in 1961 and 1963 respectively from Missouri School of Mines and Metallurgy, Rolla, Missouri. He worked for Amsted Research Laboratories, Bensenville, Illinois, as Research Metallurgist from October 1963 to December 1967. Since December 1967, he has been working for the Metallurgical Engineering Department as Research Specialist. He has also been enrolled in the Graduate School since then.

The author is married and has four children.

APPENDIX I

TABLE A

Table showing correlation between aging time and hardness at various temperatures for HM31 (Mg-3.5 wt.% Th-1.0 wt.% Mn) alloy.

Aging Temp.	260°C		280°C		300°C	
	Time (hrs)	Hardness Rockwell E Scale	Time (hrs)	Hardness Rockwell E Scale	Time (hrs)	Hardness Rockwell E Scale
	1/2	46.0	1/2	60.0	1/4	65.0
	1	59.0	1	63.0	1/2	66.0
	2	62.5	8	63.0	1	66.0
	7	67.5	24	59.5	2	67.0
	12	67.0	144	52.0	8	66.0
	19	69.0	288	47.0	12	55.0
	24	62.5	480	45.0	21	52.0
	48	60.5			30	47.0
	144	58.0			48	47.0
	336	58.0			96	48.0
	576	59.0			312	45.0
	792	59.0			480	45.0
					652	41.0
Aging Temp.	350°C		400°C			
	Time (hrs)	Hardness Rockwell E Scale	Time (hrs)	Hardness Rockwell E Scale		
	1/4	57.0	1/5	46.0		
	1/2	57.5	2/5	47.0		
	1	52.0	3/4	42.5		
	2	49.0	1	35.0		
	4	41.0	12	23.5		
	24	37.0	100	22.0		
	144	22.0	168	18.0		
	336	14.0				

APPENDIX II

TABLE A

Table showing correlation between aging time and hardness at various temperatures for HM11 (Mg-1.0 wt.% Th-1 wt.% Mn) alloy.

Aging Temp.	260°C		300°C	
	Time (hrs)	Hardness Rockwell E Scale	Time (hrs)	Hardness Rockwell E Scale
	1/3	30.0	1/2	48.0
	2/3	47.0	3/4	50.0
	1	51.5	1	53.0
	2	52.0	2 1/2	50.0
	6	54.0	7	50.0
	19	54.0	24	49.0
	90	53.0	54	42.0
	144	52.0	192	41.0
	312	53.0	336	41.0
	456	50.0	432	40.0
	734	49.5		
Aging Temp.	350°C		400°C	
	Time (hrs)	Hardness Rockwell E Scale	Time (hrs)	Hardness Rockwell E Scale
	1/5	42.5	1/5	36.0
	1/3	44.0	1/2	34.0
	1	41.0	1	32.0
	2	40.0	2	32.0
	8	35.0	6	21.5
	9	33.0	10	19.0
	24	30.0	15	8.0
	168	20.0	72	7.0
			120	6.0
			288	6.0
			480	6.0